

Deep retino-network for automatic quantification of diabetic retinopathy

Syed Amin Jameel, Abdul Rahim Mohamed Shanavas

Department of Computer Science, Jamal Mohamed College, Tiruchirappalli, India

Article Info

Article history:

Received Aug 11, 2023

Revised Dec 12, 2023

Accepted Jan 20, 2024

Keywords:

Classification system

Deep neural network

Diabetic retinopathy

Fundus image

Grading system

ABSTRACT

Diabetic retinopathy (DR) is the ocular manifestation of the systemic disease. Since it is the most prevalent cause of blindness in the world, it demands a significant amount of therapeutic attention. As a result, a precise assessment of the DR condition as well as its evolution is very important for treatment. In this work, an automated quantification of diabetic retinopathy state (AQDRS) using fundus images is proposed. The state of DR is classified into 0 (low) to 3 (high) with the help of a deep retino-network (DRN). Before the classification by DRN, an image down-sampling scheme is employed. A DRN consists of convolution layer and max-pooling layers to extract the deep retina features and fully connected layer (FCL) for AQDRS where feed-forward neural network is employed for the classification. The performance of AQDRS by DRN for grading DR is evaluated using methods to evaluate segmentation and indexing techniques in the field of retinal ophthalmology (MESSIDOR) database. Results show that the AQDRS by DRN can able to extract the relevant discriminative information for grading the fundus image. The average accuracy on normal images in MESSIDOR database is 97.9% and it is 95.3% for DR images.

This is an open access article under the [CC BY-SA](#) license.



Corresponding Author:

Syed Amin Jameel

Department of Computer Science, Jamal Mohamed College

Race Course Road, Kaja Nagar, Tiruchirappalli, Tamil Nadu 620020, India

Email: saj@jmc.edu

1. INTRODUCTION

Fundus imaging becomes the primary technique for diagnosing various eye diseases. It can be used for analyzing the blood vessels, optic nerve head, exudates and macular edema. An improved algorithm for extracting the blood vessels is discussed in [1]. It improves the conventional Gaussian filters by taking the 2nd order derivatives of it in three directions such as xx , xy , and yy . A thresholding strategy for separating the blood vessels from the maximal filter response is covered in [2]. The responses are normalized prior to applying a threshold to the greatest filter response. To identify the diabetic retinopathy (DR), the retinal vessel tortuosity is computed from the segmented blood vessels in [3]. Different algorithms are discussed that includes Hough transform, chain code, and fisher linear discrimination.

According to Badawi *et al.* [4], the tortuosity metric for DR grading is discussed. It provides an example of how to quickly identify circles for segmentation using the hough transform. The precision of the blood vessel identification technology is the primary determinant of the tortuosity measure computation. Fundus image classification techniques have recently been developed since it is very difficult to separate the blood vessels from the fundus image due to the varied illuminations. A deep learning algorithm is tested in [5] for grading DR from fundus images. It uses seven blocks of 2 layers each for deep feature extraction and weighted kappa as a loss function. For classification, a linear classifier with softmax function is used in the last

layer. An interpretable classifier is designed in [6] for grading DR. It uses a pixel wise score for every neuron and the final classification is made from the contribution of each pixel. The generated visual map helps the ophthalmologists for easy interpretation. According to Gonzalo *et al.* [7], age-related macular degeneration and an automated grading system are described. To obtain a contrast-enhanced image and a pre-processed RGB image, it employs a pre-processing stage. Three distinct deep learning architectures are used in an ensemble manner to grade DR.

Multi label classification based grading system is discussed in [8]. It visualizes pathological changes of blood vessels and optic nerve head and then diagnoses the DR grade. The retinal images are rescaled after the fundus images are enhanced and noise removed. The run length matrix features are extracted in four directions and then U-net is used for grading. According to Zhou *et al.* [9], a hybrid segmentation and classification approach for DR grading is discussed. Lesions such as soft and hard exudates, hemorrhages, and micro-aneurysms are initially segmented in the fundus image and then graded. An improved grading system using deep learning is described in [10] by the use of principal component analysis. At first the significant colour channel is selected and their principal components are calculated. Then majority voting is applied to grade DR from the results of deep learning models.

A detailed comprehensive survey of detection and DR diagnosis approaches is provided in [11]. The various available databases for DR diagnosis, machine learning approaches, DR lesion segmentation and deep learning approaches are discussed in detail. Artificial intelligence based system for DR diagnosis is described in [12] using Smartphone based fundus images. A deep learning based algorithm is designed in [13] for the detection of DR. The inception-v3 architecture is employed for the analysis. By employing parallel and concatenated convolutional layers, the inception architecture may capture intricate and multi-scale information. A prediction approach for different stages in DR is described [14]. It uses radial basis function support vector machine using different features extracted from the pre-processed fundus images for the classification.

Residual network-based DR detection is discussed in [15] using images from data augmentation. It uses transfer learning of ResNet50 for the classification. It is a 50-layer architecture with residual connection for faster learning and effective classification. Inceptionv3 architecture is employed in [16] for DR classification. From the segmented image by fuzzy c-mean clustering, co-occurrence features are extracted. Inception networks are a popular choice for computer vision problems because they have been crucial in lowering computational costs while enhancing model accuracy. A detailed review of DR classification techniques by Bayesian deep learning methods is provided in [17]. A deep convolution neural network discussed in [18] classifies the DR images into five classes. A comparative analysis of different machine learning algorithms used for DR classification is provided in [19].

Problem statement: with the assistance of traditional classification systems like k -nearest neighbor, support vector machine, decision trees, naive Bayes, and random forest classifiers, a broad range of automated approaches have been developed. These methods are based on textural properties of fundus images. The accuracy of traditional classification systems is reliant on the features that are extracted as well as the classifiers that are chosen. Both the prominent characteristics may fail due to the poor classifier and vice versa. In addition, the creation of an accurate categorization system necessitates the use of two distinct modules.

Solution: in recent years, many architectural frameworks based on deep learning have been developed for different applications that avoid separate feature extraction stage for the classification. The visual geometric group (VGG) [20], ResNet [21], and AlexNet [22] have made significant contributions to the field of computer vision. Each of these designs has its unique set of properties and has been important in various computer vision tasks, including image classification. The main objective of this work is to create an efficient architecture capable of providing an accurate and dependable classification of DR stages by making use of fundus images.

Results: the performance of the proposed deep retino-network (DRN) architecture is tested on MESSIDOR database and it gives average accuracy of 97.9% on normal images and 95.3% for DR images. A novel DRN design is discussed briefly in this paper which improves the efficiency of the grading system. The paper organization is as follows: the proposed automated quantification of diabetic retinopathy state (AQDRS) system is discussed in section 2 with the DRN design and the down sampling scheme. In section 3, the characteristics of database images and the detailed evaluation of the system are discussed. The last section summarizes the proposed AQDRS system.

2. METHODS AND MATERIALS

In this section, an automatic grading system is discussed based on the DRN. The proposed AQDRS system is shown in Figure 1. It consists of a down-sampling scheme for dimension reduction and the proposed DRN for the classification. Prior to the classification by DRN, the fundus images are down-sampled to a fixed resolution as the database has fundus images with different resolutions.

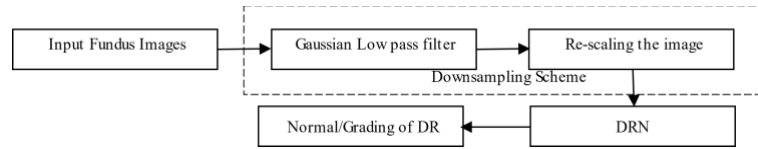


Figure 1. Proposed AQDRS system

2.1. Down-sampling scheme

There are two main tasks involved in designing an image down-sampling scheme. The first task is selecting the filtering method. Here the Gaussian low-pass filtering [23] is chosen as it is commonly used. The second task is to determine the size of the down-sampling process. In the field of signal and image processing, Gaussian low-pass filter is often used. It eliminates high-frequency noise while still maintaining the integrity of the low-frequency information.

A Gaussian filter is a smoothing filter that uses a Gaussian function as the weighting function for averaging the neighboring pixel values. The Gaussian function is a bell-shaped curve with the highest value at the centre and quickly dropping away from the centre. It is symmetrical about the centre point and is also known as the Gaussian distribution. The formula for a one-dimensional Gaussian function is:

$$p(z) = \frac{1}{\sigma\sqrt{2\pi}} e^{-\frac{(z-\mu)^2}{2\sigma^2}} \quad (1)$$

Where σ is the standard deviation of Gaussian distribution with mean (μ). To apply a Gaussian filter to an image, the Gaussian kernel is convolved with the images at different points. The size of the kernel and the value of sigma determine the strength and extent of the smoothing effect. The resolution of the down-sampled image determines the computational complexity of the DRN. If the image size is smaller, it would take less time to extract deep features and training the network. After determining the down-sampling scheme, the original image is convolved with the low-pass filter first. Then it is down-sampled to obtain an image of reduced size (256×256 pixels) by Bicubic interpolation [24].

2.2. Deep retino network

A DRN consists of convolution layer and max-pooling layers to extract the deep retina features and fully connected layer (FCL) for AQDRS. Figure 2 shows the proposed DRN for AQDRS system. A convolution layer is a fundamental building block in convolutional neural networks (CNNs). It performs convolution operation on the input data, which is typically an image, to extract features that are relevant to the task at hand. The weights of the kernel are learned through backpropagation during the training process, with the goal of optimizing some objective function, such as accuracy or loss. Convolution layers typically consist of multiple kernels, each of which produces a separate feature map. The number of kernels in a convolution layer is a hyper-parameter of the network, and determines the number of features that the network can learn. Deep learning architectures for different applications differ in their arrangement of layers [25]–[28]. It uses a simple arrangement with convolution filter of size 3×3 and max pooling layer of size 2×2 with stride 2. The output of a convolution layer is often passed through an activation function, such as rectified linear unit (ReLU), to introduce non-linearity into the network.

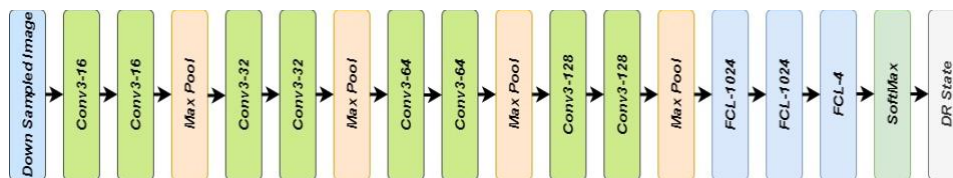


Figure 2. Proposed DRN for AQDRS system

The max-pooling layer works to diminish the higher dimension space which is produced by the convolution layer. It is a form of down-sampling procedure that separates the input data into rectangular sections that do not overlap with one another and then outputs the value that is highest inside each of those regions. As the max pooling layer uses stride of 2, the high dimension space is reduced to half of its size and

then passed to the next convolution layer and the ReLU activation is used in each convolution layer. Figure 3 shows the computation of max-pooling layer. Figure 3(a) shows the sample 4×4 input and Figure 3(b) shows the max-pooled output.

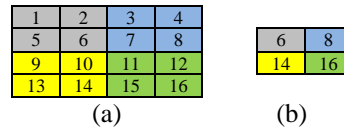


Figure 3. Computation of max-pooling layer (a) input and (b) max-pooled output

A FCL or dense layer is a type of artificial neural networks. In an FCL, every neuron in the layer is linked to every neuron in the previous layer. The output of each neuron in the FCL is computed by first taking a weighted sum of the inputs, then applying an activation function. Figure 4 shows a simple feed forward neural network.

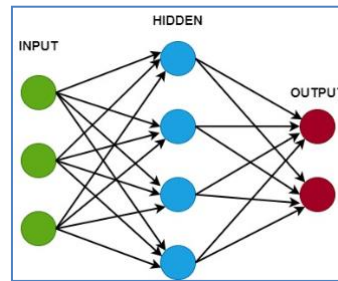


Figure 4. Feed forward network

In DRN, the FCL consists of a multilayered feed forward neural network which is a hierarchical arrangement of large number of nodes with adaptive weights (w). A weighted sum of the inputs is performed by each node in a hidden layer, and a non-linear modification of that total, coupled with a bias, is generated by that node (b). The back-propagation algorithm continues to be the most common choice for training neural networks despite the fact that it is not the most efficient. It is a process used to repeatedly update the weights such that the weight is proportional to the derivative of the error function such that.

$$w_{nm(new)} = w_{nm(old)} + \Delta w_{nm} \quad (2)$$

where $\Delta w_{nm} = -\eta \frac{\partial E}{\partial w_{nm}}$. The instantaneous sum squared error between the actual and target outputs is given in (3)

$$E = \frac{1}{2} \sum_{i=1}^n (t_i - o_i)^2 \quad (3)$$

where n is the number of classes or nodes in the output layer. The error function can also be written as (4):

$$E = \frac{1}{2} \sum_{i=1}^m \{t_i - f_i(net_i)\}^2 \quad (4)$$

where:

$$net_i = \sum_{j=1}^m w_{ij} o_{j+b} \quad (5)$$

and:

$$f_i(net_i) = \frac{1}{1 + e^{-\beta net_i}} \quad (6)$$

Where m is the number of nodes in the hidden layer, β is the slope of the sigmoid function, and b is the bias. It is assumed that the bias is a weight that is associated to a node and has an activation value that is always set

to one. After this, the bias is updated in a manner that is analogous to how the other weights are modified. The summation in (5) can be expressed as $net_i = \sum_{j=1}^m w_{ij}o_j$. In a single layer hidden network as in Figure 5, the error is computed as in (7)

$$E = \frac{1}{2} \sum_{i=1}^n \{t_i - f_i(\sum_{j=0}^m w_{ij}f_j(\sum_{k=0}^l w_{jk}x_k))\}^2 \quad (7)$$

The evaluation of weights (Δw) is straightforward and can be written as (8):

$$\Delta w_{nm} = -\eta \frac{\partial E}{\partial w_{nm}} [\sum_{i=1}^n \{t_i - f_i(\sum_{j=0}^m w_{ij}f_j)\}^2] \quad (8)$$

It is already stated that the backpropagation algorithm can employed to train a neural network by minimizing the average squared error energy over all the training samples. Neural networks may effectively capture and learn complicated patterns and correlations by using the hidden layers with nonlinear activation functions. This allows the input data to be transformed into a high-dimensional space. Hence, neural networks are capable of efficiently solving many tasks, such as image classification, natural language processing, and reinforcement learning.

3. RESULTS AND DISCUSSIONS

The performance of AQDRS by DRN for grading DR is evaluated by using the standard set of fundus images available in MESSIDOR database [29], [30]. It consists of 1,200 images (800 images with pupil dilation and 400 images without dilation). All images are graded into 4 classes of DR; normal (625 images), DR-1 (197 images), DR-2 (130 images), DR-3 (248 images). All images are in TIFF format with three different resolutions; 2,240×1,488, 1,440×960, and 2,304×1, 536 pixels. The experiments on MESSIDOR database are evaluated in terms of average accuracy and accuracy of individual categories. Sample images are shown in Figure 5. Figures 5(a) and 5(b) show two sample fundus images of the normal and DR-1 categories. Figures 5(c) and 5(d) show the DR-2 and DR-3 category images.

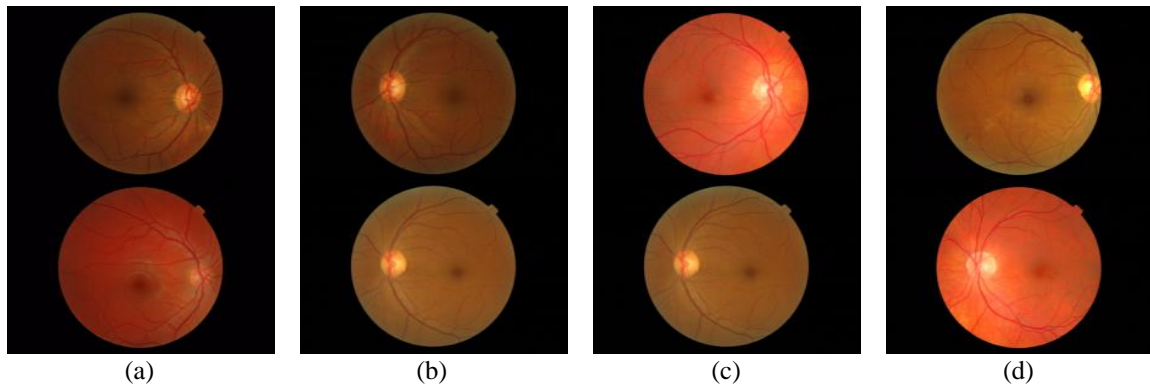


Figure 5. Samples in the MESSIDOR database (a) normal (b) DR-1 (c) DR-2 (d) DR-3

To show the efficiency, the performance of the proposed AQDRS is compared with the ground truth data in the MESSIDOR database. The hyper-parameters of the proposed DRN system for AQDRS are shown in Table 1. Based on the results of AQDRS and the ground truth data, the confusion matrix is formed for the multi-classification. It is shown in Table 2. Table 3 shows the performance of the AQDRS with DR and no-DR fundus images.

Table 1. Hyper-parameters of the proposed system

Hyper parameter	Value	Hyper parameter	Value
Mini Batch Size	32	Learn rate- Drop factor	0.4
No. of epochs	50	Learn rate- Drop Period	3
Initial learning rate	3e ⁻⁴	L2 regularization	0.0005
Learn rate reschedule	Piecewise	Validation frequency	50

Table 2. Performance of AQDRS system on MESSSIDOR fundus images of all categories

Confusion Matrix (Multi Classification)		Prediction by AQDRS			
		Normal	DR-0	DR-1	DR-3
MESSIDOR ground truth data	Normal	612	27	0	0
	DR-0	8	145	6	0
	DR-1	5	23	118	8
	DR-2	0	2	6	240
Total		625	197	130	248

Table 3. Performance of AQDRS system on MESSSIDOR fundus images of all grades of DR and normal images

Confusion Matrix (Binary Classification)		Prediction by AQDRS	
		Normal	DR
MESSIDOR ground truth data	Normal	612	27
	DR	13	548
Total		625	575

Based on the outputs in the Tables 2 and 3, the performances of AQDRS system are analyzed in terms of sensitivity, specificity, and accuracy. Table 4 shows the performance of AQDRS system for binary classification. It can be seen from Table 4 that the accuracy of the AQDRS for the classification of normal images is 97.9% (specificity) and DR images is 95.3% (sensitivity). The average classification accuracy of AQDRS is 96.67%. Table 5 shows the performance of AQDRS system for multi classification.

Table 4. Performance metrics of AQDRS system for binary classification

Classification method	Performance metrics		
	Sensitivity	Specificity	Accuracy
Binary classification	95.30	97.92	96.67

Table 5. Performance metrics of AQDRS system for multiclass classification

Multi classification	Performance metrics		
	Sensitivity	Specificity	Accuracy
Normal	97.92	95.30	96.67
DR-0	93.60	95.60	94.50
DR-1	90.77	96.64	96.00
DR-2	96.77	99.16	98.67

It can be seen from Table 5 that the individual accuracies for each grade are 94.5% (DR-0), 96.00% (DR-1) and 98.67% (DR-2). It is observed that the AQDRS system has 96.67% accuracy for the classification of normal fundus images. A comparative analysis with other state-of-art deep learning architectures is provided in Figure 6. It can be seen from Figure 6 that the proposed AQDRS system has the highest sensitivity of 94.76%, followed closely by AlexNet [22] at 92.24%. Specificity is also highest in the proposed system at 96.67%, with AlexNet [22] close behind at 94.52%. The proposed AQDRS system demonstrates a significant advantage over other architectures, achieving 96.46% of overall accuracy, while VGG [20] and ResNet [21] attain 90.23% and 91.52%, respectively. These results suggest that the proposed system outperforms the other models, making it a best performer for DR classification.

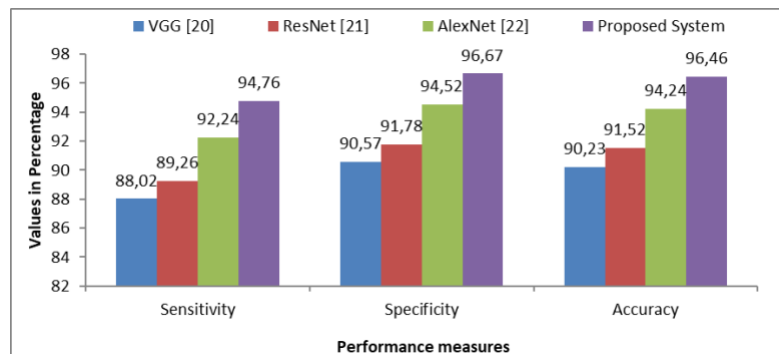


Figure 6. Comparative analysis of proposed AQDRS system with state-of-art architectures

4. CONCLUSION

In this paper, a complete and fully automated grading system for DR is presented. It performs all the necessary tasks including deep feature extraction and classification. The proposed arrangement of convolution layers and pooling layers perform the deep feature extraction and the resulting features are then classified using feed forward neural network. Results show that the DRN has the ability to grade the fundus images. Moreover, it could identify the normal images as well from the deep features. Also, it is noted that there is no need for manual intervention for grading the DR. In future, the performance of the AQDRS system to classify the mild DR can be improved by fine tuning the arrangements of the DRN and including exact pre-processing techniques which shows the structures of DR effectively.




REFERENCES

- [1] Maison, T. Lestari, and A. Luthfi, "Retinal blood vessel segmentation using gaussian filter," *Journal of physics: conference series*, vol. 1376, no. 1, pp. 1–5, 2019, doi: 10.1088/1742-6596/1376/1/012023.
- [2] K. Wisaeng, "Retinal blood-vessel extraction using weighted kernel fuzzy c-means clustering and dilation-based functions," *Diagnostics*, vol. 13, pp. 1–21, 2023, doi: 10.3390/diagnostics13030342
- [3] S. A. Q. Badawi, M. Takturi, Y. Albadawi, M. A. K. Khatkhat, A. K. Nileseshwar, and E. Mosalam, "Four severity levels for grading the tortuosity of a retinal fundus image," *Journal of Imaging*, vol. 8, no. 10, pp. 1–19, 2022, doi: 10.3390/jimaging8100258.
- [4] S. A. Badawi *et al.*, "Detection and grading of hypertensive retinopathy using vessels tortuosity and arteriovenous ratio," *Journal of Digital Imaging*, vol. 35, pp. 281–301, 2022, doi: 10.1007/s10278-021-00545-z.
- [5] M. B. Bernaldiz *et al.*, "Testing a deep learning algorithm for detection of diabetic retinopathy in a spanish diabetic population and with messidor database," *Diagnostics*, vol. 11, no. 8, Jul. 2021, doi: 10.3390/diagnostics11081385.
- [6] J. D. L. Torre, A. Valls, and D. Puig, "A deep learning interpretable classifier for diabetic retinopathy disease grading," *Neurocomputing*, vol. 396, pp. 465–476, 2020, doi: 10.1016/j.neucom.2018.07.102.
- [7] C. G. Gonzalo *et al.*, "Evaluation of a deep learning system for the joint automated detection of diabetic retinopathy and age-related macular degeneration," *Acta Ophthalmologica*, vol. 98, no. 4, pp. 368–377, Jun. 2020, doi: 10.1111/aos.14306.
- [8] E. Abdelmaksoud, S. E. -Sappagh, S. Barakat, T. Abuhmed, and M. Elmogy, "Automatic diabetic retinopathy grading system based on detecting multiple retinal lesions," *IEEE Access*, vol. 9, pp. 15939–15960, 2021, doi: 10.1109/ACCESS.2021.3052870.
- [9] Y. Zhou, B. Wang, L. Huang, S. Cui, and L. Shao, "A benchmark for studying diabetic retinopathy: segmentation, grading, and transferability," *IEEE Transactions on Medical Imaging*, vol. 40, no. 3, pp. 818–828, 2021, doi: 10.1109/TMI.2020.3037771.
- [10] E. Mohamed, M. A. Elmohsen, and T. Basha, "Improved automatic grading of diabetic retinopathy using deep learning and principal component analysis," *Proceedings of the Annual International Conference of the IEEE Engineering in Medicine and Biology Society, EMBS*, IEEE, pp. 3898–3901, 2021, doi: 10.1109/EMBC46164.2021.9630919.
- [11] V. Lakshminarayanan, H. Kheradfallah, A. Sarkar, and J. J. Balaji, "Automated detection and diagnosis of diabetic retinopathy: a comprehensive survey," *Journal of Imaging*, vol. 7, no. 9, Aug. 2021, doi: 10.3390/jimaging7090165.
- [12] S. Gupta, S. Thakur, and A. Gupta, "Optimized hybrid machine learning approach for smartphone based diabetic retinopathy detection," *Multimedia Tools and Applications*, vol. 81, pp. 14475–1450, 2022, doi: 10.1007/s11042-022-12103-y.
- [13] F. Li, Z. Liu, H. Chen, M. Jiang, X. Zhang, and Z. Wu, "Automatic detection of diabetic retinopathy in retinal fundus photographs based on deep learning algorithm," *Translational Vision Science and Technology*, vol. 8, no. 6, Nov. 2019, doi: 10.1167/tvst.8.6.4.
- [14] M. K. Behera, "Prediction of different stages in diabetic retinopathy from retinal fundus images using radial basis function based SVM," *Indian Journal of Science and Technology*, vol. 13, no. 20, pp. 2030–2040, 2020, doi: 10.17485/ijst/v13i20.322.
- [15] Y. S. Devi, and S. P. Kumar, "A deep transfer learning approach for identification of diabetic retinopathy using data augmentation," *IAES International Journal of Artificial Intelligence*, vol. 11, no. 4, pp. 1287–1296, 2022, doi: 10.11591/ijai.v11.i4.pp1287-1296.
- [16] T. T. Ramanathan, M. J. Hossen, M. S. Sayeed, and J. E. Raja, "A deep learning approach based on stochastic gradient descent and least absolute shrinkage and selection operator for identifying diabetic retinopathy," *Indonesian Journal of Electrical Engineering and Computer Science*, vol. 25, no. 1, pp. 589–600, 2022, doi: 10.11591/ijeecs.v25.i1.pp589-600.
- [17] H. R. Ismail, and M. M. Hassan, "Bayesian deep learning methods applied to diabetic retinopathy disease: a review," *Indonesian Journal of Electrical Engineering and Computer Science*, vol. 30, no. 2, pp. 1167–1177, 2023, doi: 10.11591/ijeecs.v30.i2.pp1167-1177.
- [18] L. Akshita, H. Singhal, I. Dwivedi, and P. Ghuli, "Diabetic retinopathy classification using deep convolutional neural network," *Indonesian Journal of Electrical Engineering and Computer Science*, vol. 24, no. 1, pp. 208–216, 2021, doi: 10.11591/ijeecs.v24.i1.pp208-216.
- [19] K. Kangra, and J. Singh, "Comparative analysis of predictive machine learning algorithms for diabetes mellitus," *Bulletin of Electrical Engineering and Informatics*, vol. 12, no. 3, pp. 1728–1737, 2023, doi: 10.11591/eei.v12i3.4412.
- [20] K. Simonyan and A. Zisserman, "Very deep convolutional networks for large-scale image recognition," *Arxiv-Computer Science*, pp. 1–14, 2015.
- [21] K. He, X. Zhang, S. Ren, and J. Sun, "Deep residual learning for image recognition," *Proceedings of the IEEE Computer Society Conference on Computer Vision and Pattern Recognition*, pp. 770–778, 2016, doi: 10.1109/CVPR.2016.90.
- [22] A. Krizhevsky, I. Sutskever, and G. E. Hinton, "ImageNet classification with deep convolutional neural networks," *Communications of the ACM*, vol. 60, no. 6, pp. 84–90, 2017, doi: 10.1145/3065386.
- [23] R. S. Kadurka, and H. Kanakalla, "Automated bird detection in audio recordings by a signal processing perspective," *International Journal of Advances in Signal and Image Sciences*, vol. 7, no. 2, pp. 11–20, 2021, doi: 10.29284/ijasis.7.2.2021.11-20.
- [24] S. J. Devaraj, "Emerging paradigms in transform-based medical image compression for telemedicine environment," *Telemedicine Technologies*, pp. 15–29, 2019, doi: 10.1016/B978-0-12-816948-3.00002-7.
- [25] M. A. Ramitha, and N. Mohanasundaram, "Classification of pneumonia by modified deeply supervised resnet and senet using chest x-ray images," *International Journal of Advances in Signal and Image Sciences*, vol. 7, no. 1, pp. 30–37, 2021, doi: 10.29284/ijasis.7.1.2021.30-37.
- [26] N. Veni, and J. Manjula, "Modified visual geometric group architecture for MRI brain image classification," *Computer Systems Science and Engineering*, vol. 42, no. 2, pp. 825–835, 2021, doi: 10.32604/CSSE.2022.022318.
- [27] S. P. Maniraj, and P. Sardarmaran, "Classification of dermoscopic images using soft computing techniques," *Neural Computing and Applications*, vol. 33, no. 19, pp. 13015–13026, 2021, doi: 10.1007/s00521-021-05998-5.




- [28] A. S. A. Hans, and S. Rao, "A CNN-LSTM based deep neural networks for facial emotion detection in videos," *International Journal of Advances in Signal and Image Sciences*, vol. 7, no. 1, pp. 11–20, 2021, doi: 10.29284/ijasis.7.1.2021.11-20.
- [29] E. Decencière *et al.*, "Feedback on a publicly distributed image database: the messidor database," *Image Analysis and Stereology*, vol. 33, no. 3, pp. 231–234, 2014, doi: 10.5566/ias.1155.
- [30] J. Krause *et al.*, "Grader variability and the importance of reference standards for evaluating machine learning models for diabetic retinopathy," *Ophthalmology*, vol. 125, no. 8, pp. 1264–1272, 2018, doi: 10.1016/j.ophtha.2018.01.034.

BIOGRAPHIES OF AUTHORS



Dr. Syed Amin Jameel    is working as Assistant Professor, P.G & Research Department of Computer Science, Jamal Mohamed College (Autonomous), Tiruchirappalli, Tamil Nadu, India. Affiliated to Bharathidasan University, Tiruchirappalli-620 024. He completed his Ph.D. degree in Computer Science in December 2017. He has 23 years of UG and PG teaching experience. He has published 10 research papers in reputed journals. He has presented 25 papers in national and international conferences. He has participated in many seminars, workshops and conferences. He guided 17 M.Phil. Research Scholars. His area of interest is computer graphics and image processing. He is an approved Doctoral Committee Member of Bharathidasan University. He is a Member of International Association of Computer Science and Information Technology, Singapore, International Association of Engineers, Hong Kong and Computer Science Teachers Association, U.S.A. He can be contacted at email: saj@jmc.edu.



Dr. Abdul Rahim Mohamed Shanavas    is working as an Associate Professor, Department of Computer Science, Jamal Mohamed College, Tiruchirappalli, Tamil Nadu, India. Affiliated to Bharathidasan University, Tiruchirappalli-620 024. He completed his Ph.D. degree in February 2010. He has 34 years of UG and PG teaching experience. He has published twenty-two research articles in reputed journals. He has presented 7 articles in national and international conferences. He has participated in many seminars, workshops and conferences and also acted as a resource person. He is the Dean of Science and Coordinator of Student Monitoring committee. He guided 100+ M.Phil. Research scholars. Twelve research scholars have completed their Ph.D. under his guidance. At present seven scholars are pursuing their Ph.D under his guidance. His area of interest is computer graphics and image processing. He is an approved Research Advisor of Bharathidasan University, Tiruchirappalli and Bharathiar University, Coimbatore. He can be contacted at email: arms3375@gmail.com.